



Cite this: *Anal. Methods*, 2017, 9, 2452

# Electrochemiluminescent detection of glyphosate using electrodes modified with self-assembled monolayers

Gabriela Marzari, Maria V. Cappellari, Gustavo M. Morales and Fernando Fungo \*

The use of glyphosate (GlyP) in agriculture has caused environmental and health concerns in modern society. Even today, its quantification remains an analytical challenge. Therefore, the development of analytical methods is required that allows an increase in sample throughput and cost-savings. This study presents a study of the electrochemiluminescence (ECL) behaviour of the GlyP/Ru(bpy)<sub>3</sub><sup>2+</sup> system on gold electrodes modified with self-assembled monolayers (SAM). The ECL response was analysed on three different electrode surfaces, bare gold and alkyl-thiol monolayers with ionizable (–COOH) and non-ionizable (–CH<sub>3</sub>) terminal group. It was found that the ECL signal of the GlyP/Ru(bpy)<sub>3</sub><sup>2+</sup> system was improved by the modification of the electrodes reaching a limit of quantification (LOQ) of 6.42 μM when the SAM contained a carboxylic end-group. In addition, the effect of the electrodes modification on the ECL behaviour is discussed. The results obtained and the calculated analytical parameters show the potential of the proposed method to determine GlyP.

Received 24th February 2017

Accepted 28th March 2017

DOI: 10.1039/c7ay00506g

rsc.li/methods

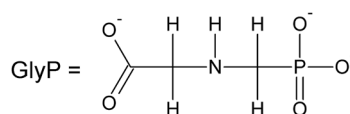
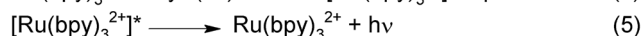
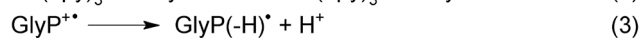
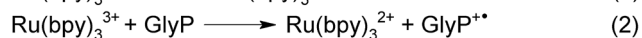
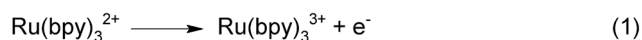
## Introduction

Modern agriculture demands the utilization of new technological tools that allow an effective weed control based on the use of transgenic crop varieties resistant to herbicides.<sup>1–3</sup> The global spread of these agricultural practices have led to the massive use of artificially modified green species, herbicides and pesticides on an unprecedented scale. As a result, the development of methods and technologies for evaluating the environmental impact of farming practices is extremely important.<sup>4,5</sup> One of the most extensively utilized herbicides worldwide is glyphosate, *N*-(phosphonomethyl)glycine (Scheme 1). Glyphosate (GlyP) has physicochemical characteristics of low molecular weight, low volatility, high polarity, amphoteric behaviour and absence of chromophores that make its detection an analytical challenge.<sup>6</sup> Currently, most of the analytical methods used to quantify GlyP require chemical derivatization, which is expensive in terms of time and money, making it difficult to measure GlyP in large amounts of samples.<sup>6</sup> For example, gas chromatography coupled to mass spectrometry is sensitive, but this detection method requires derivatization of ionic groups. Liquid chromatography is adequate for ionisable groups; however, the lack of chromophores in GlyP does not allow the use of spectroscopic techniques such as fluorescence and UV absorption.<sup>6</sup>

Therefore, the development of analytical techniques that allow the detection of GlyP is of great importance to study the impact of agricultural production on the environment.

However, there are only a few examples on the development of new methods for the detection of GlyP that do not require chemical derivatization.<sup>7–10</sup>

ECL is the process where electrochemically generated species undergo electron-transfer reactions to form excited states that emit light (luminophore species or emitter). A co-reactant is a compound that, upon oxidation, produces strong reducing intermediates, which can react with the luminophore to generate excited states that emit light (oxidative reduction mechanism). The use of the co-reactants in aqueous solution allows to overcome the problems associated with the narrow electrochemical windows of water. Essentially, there are commercially available ECL analytical instruments based on co-reactant ECL technology.<sup>11</sup> Typically used ECL luminophores and co-reactants are Ru complexes and aliphatic amines



**Scheme 1** Proposed ECL reaction mechanism of GlyP/Ru(bpy)<sub>3</sub><sup>2+</sup> system at glassy carbon electrodes.<sup>20</sup>

Department of Chemistry, Universidad Nacional de Río Cuarto-CONICET, Ruta Nac. 36 – Km. 601, X5804BYA, Argentina. E-mail: f.fungo@exa.unrc.edu.ar



derivatives, respectively.<sup>12</sup> As shown in Scheme 1, GlyP has a secondary alkylamine that can give it co-reactants properties. Therefore, ECL has the potential to provide a sensitive, rapid, and reliable detection of GlyP at low concentrations and costs. Thus, ECL can complement the existing GlyP detection techniques as a first estimation test. Currently, a few methods have been reported for the quantitation of GlyP using ECL at carbon electrodes.<sup>13–19</sup> In 1997, Ridlen *et al.* reported a quantitative analysis of GlyP and some structurally related compounds using tris(2,2'-bipyridyl)ruthenium(II) ( $\text{Ru}(\text{bpy})_3^{2+}$ ) electrogenerated chemiluminescence (ECL).<sup>13</sup> This analytical method had a detection limit of 0.01  $\mu\text{M}$  for GlyP with a linear working range of five orders of magnitude. In 2010, Jin *et al.* studied ECL for the GlyP/ $\text{Ru}(\text{bpy})_3^{2+}$  system with the aim of obtaining information about the kinetics and possible reaction pathways involved in the ECL process (Scheme 1).<sup>20</sup> They found that the ECL intensity of this system strongly depended on the media pH and proposed a catalytic homogeneous electron transfer between  $\text{Ru}(\text{bpy})_3^{3+}$  and GlyP as the rate determining step to produce the light emitting species  $[\text{Ru}(\text{bpy})_3^{2+}]^*$  (step 2, Scheme 1).

This study reports the ECL performance of the GlyP/ $\text{Ru}(\text{bpy})_3^{2+}$  system on gold electrodes modified with self-assembled monolayers (SAM) of alkanethiol derivatives with the aim of studying its electroluminescent behaviour. The use of SAM allows the designing of electrodes with controllable surface properties by introducing different terminal group chemical functionalities. The ability to control and manipulate the surface properties of conventional metal electrodes using SAM can lead to enhanced selectivity, sensitivity and/or reproducibility in electrochemical sensors.<sup>21–23</sup> To analyse the hydrophilic–hydrophobic and electrostatic interactions of the electrode surface with the system GlyP/ $\text{Ru}(\text{bpy})_3^{2+}$  and its effect on the ECL signal, two different types of alkanethiols were used to form the SAM. Thus, were studied two SAM modified electrodes, one formed by dodecanethiol that contains a non-ionizable hydrophobic terminal group (hereafter Au/SAM- $\text{CH}_3$ ) and another formed by a mixture of 1-dodecanethiol and 11-mercaptoundecanoic acid, which holds an ionizable hydrophilic terminal group (hereafter Au/SAM-COOH). It was found that the level of quantification of GlyP in phosphate buffer solution by ECL could be improved by designing the surface of the electrode. The results show that Au/SAM electrodes have the potential to be used as an ECL sensor in environmental and biological analysis.

## Experimental

### General

1-Dodecanethiol  $\geq 98\%$  (DDT, Sigma-Aldrich), 11-mercaptoundecanoic acid 98% (MUA, Sigma-Aldrich), and tris(2,2'-bipyridyl)ruthenium(II) chloride hexahydrate 99.95% (Sigma-Aldrich) were used without further purification. Analytical grade chemicals including NaOH,  $\text{Na}_2\text{HPO}_4$  and  $\text{NaH}_2\text{PO}_4$  were used as received. Absolute ethanol (Merck) and type I quality water (ELGA, PURELAB Classic) were used for all the experiments.

### Electrochemical characterizations

The electrochemical characterizations were performed with a CHI Model 600E series electrochemical analyser (CH Instruments, Inc. Texas, USA). A conventional three-electrode cylindrical Pyrex electrochemical cell (diameter: 20 mm and high: 130 mm) featured an inlaid polycrystalline Au disk (diameter: 2 mm) as the working electrode, a platinum coil as the counter electrode, and mercury/mercurous sulfate (saturated  $\text{K}_2\text{SO}_4$ , MSRE) as a reference electrode. All potentials were reported against the Standard Hydrogen Electrode (SHE) using  $-0.64\text{ V}$  as a scale conversion factor.<sup>24</sup> The electrochemical experiments were carried out in approximately 3 mL of 0.1 M phosphate buffer at pH 8. The settings used for the observations of differential pulse voltammograms (DPVs) were as follows: 2 s quiet time, 0.004 V increment potential, 0.05 V amplitude, 0.05 s pulse width, 0.02 s sample width, and 0.5 s pulse period. All measurements were made at room temperature and under an argon atmosphere.

### Electrogenerated chemiluminescence (ECL)

The ECL experiments were carried out using the same electrodes and conditions for the electrochemical experiments in a homemade cylindrical PTFE cell (diameter 15 mm and height 57 mm) with an optically flat Pyrex glass at the cell bottom. The ECL cell was mounted in a homemade holder placed on an optical rail. The platinum wire counter electrode was covered in order to avoid the detection of spurious ECL. The ECL signals were recorded with a photomultiplier (PMT, Mod. Hamamatsu H7467-01), and the electrochemical cell and PMT were both inside of a homemade black box. The PMT was operated in photon counting mode, which improved the signal/noise ratio compared to that in analogue mode. Data transfer, and other necessary settings were controlled by software, which was specially designed in our laboratory through an RS-232C interface. The ECL signals were generated by applying steps or a square wave voltage waveform to the working electrode. The ECL calibration curves were obtained from 0 to 100  $\mu\text{M}$  for GlyP in the presence of 0.1 mM  $\text{Ru}(\text{bpy})_3^{2+}$ . The plotted ECL values used to build the GlyP calibration curve were the average integrated areas of three consecutive ECL peaks obtained by three potential steps between 0.0 V and 1.25 V, with a pulse width of 0.1 s and a quiet time of 1 s between steps. Each point in the calibration curve was measured in duplicate, and the electrode was cleaned and reconditioned between determinations by cycling the potential in buffer solutions.

### Preparation of substrates and monolayers

Prior to each experiment, the Au electrode was mechanically polished on felt with an alumina suspension (0.3  $\mu\text{m}$ ) and then sonicated and rinsed with deionized water several times. Subsequently, the electrodes were electrochemically polished using 25 successive scans between  $-0.4\text{ V}$  and  $1.0\text{ V}$  vs. MSRE in 0.5 M  $\text{H}_2\text{SO}_4$  aqueous solution, at  $0.1\text{ V s}^{-1}$ . Finally, the electrodes were rinsed with copious amounts of water and absolute ethanol and immediately placed in thiol solution. The



monolayers were assembled by spontaneous adsorption of the thiols from a solution in absolute ethanol free of oxygen at room temperature. Both the pure and two-component thiol SAMs were prepared by immersing the Au electrode previously cleaned in the ethanol solution containing DDT and DDT/MUA in a 1 : 1 molar ratio for 12 h. The total concentration of the thiols in the solution was kept constant at 1 mM. Upon removal from the thiol solution, the electrodes were rinsed in absolute ethanol and then with phosphate buffer solution.<sup>25,26</sup> All the experiments were performed with freshly prepared modified electrodes.

## Results and discussion

### Electrochemical characterization

Electrochemical experiments were performed to analyse the individual redox behaviour of  $\text{Ru}(\text{bpy})_3^{2+}$  and GlyP on bare Au and electrodes modified by SAM. Fig. 1 summarizes the differential pulse voltammograms (DPVs) that were obtained for  $\text{Ru}(\text{bpy})_3^{2+}$  and GlyP on a bare Au electrode, respectively. The dashed curves in both figures indicate the typical voltammetric behaviour observed for a polycrystalline gold electrode in aqueous basic media.<sup>27,28</sup> The DPV in Fig. 1a shows a reversible oxidation process (indicated with vertical arrows) mounted on the gold oxide formation wave with a peak potential at 1.28 V, which was assigned to the electrochemical oxidation of  $\text{Ru}(\text{bpy})_3^{2+}$  in aqueous solution.<sup>11,23</sup> On the other hand, Fig. 1b shows the DPV obtained for the buffer solution containing GlyP, where a redox response associate to GlyP was not distinguished from the electrochemical background of the Au electrode. This observation, in agreement with previous electrochemical studies of alkyl amine derivatives and GlyP, indicates that the oxidation of GlyP occurs at potentials beyond the electrochemical window of the electrolyte solution.<sup>11,20,29</sup>

Moreover, the DPV obtained for  $\text{Ru}(\text{bpy})_3^{2+}$  in phosphate buffer on an Au electrode modified with a SAM formed by 1-dodecanethiol ( $\text{Au}/\text{SAM}-\text{CH}_3$ ) are shown in Fig. 2a.

As expected, the  $\text{SAM}-\text{CH}_3$  effectively blocked the oxide formation on the Au electrode surface (see dashed line).<sup>23,30</sup> However, the  $\text{Ru}(\text{bpy})_3^{2+}$  redox response was clearly visible regarding the background line with a wave centred at 1.27 V. This behaviour is in agreement with previous reports for this electroactive species in aqueous solution on a glassy carbon electrode.<sup>20</sup> Unlike the previously observed results for bare Au electrode in Fig. 1a, the prevention of the formation of surface oxides through the SAM protective effect clearly allowed the electrochemical oxidation of  $\text{Ru}(\text{bpy})_3^{2+}$  to be observed.<sup>31</sup> However, when the applied potential was above  $\sim 1.38$  V, the current density significantly increased due to the oxidation of the thiol–Au bond (see dashed line) and consequently, the  $\text{SAM}-\text{CH}_3$  started to desorb from the metal surface.<sup>32</sup> This modified electrode had an electrochemical window (approximately  $\sim 0.5$  V, see red dashed line in Fig. 1) smaller than that of the bare Au electrode. Therefore, it was also not possible to reach the GlyP oxidation potential. However, taking into account that the ECL generation with the  $\text{Ru}(\text{bpy})_3^{2+}/\text{GlyP}$  system was initiated with the  $\text{Ru}(\text{bpy})_3^{2+}$  oxidation (see Scheme 1), it is possible to assume that  $\text{Au}/\text{SAM}-\text{CH}_3$  has the potential to be an ECL active electrode in the presence of GlyP.

The Au electrode surface modified with a binary combination of MUA and DDT (from here denoted as  $\text{Au}/\text{SAM}-\text{COOH}$ ) showed similar electrochemical behaviour to that of  $\text{Au}/\text{SAM}-\text{CH}_3$ .<sup>25</sup> In the voltammogram of Fig. 2b is observed that gold oxide formation is inhibited and a clear wave corresponding to the electro-chemical oxidation of  $\text{Ru}(\text{bpy})_3^{2+}$  is detected. However, the faradaic current density is higher than that observed in  $\text{Au}/\text{SAM}-\text{CH}_3$  (Fig. 2a). This behaviour can be associated to the presence of an ionizable  $-\text{COOH}$  group, which interacts with the electrolyte affecting the double layer charging

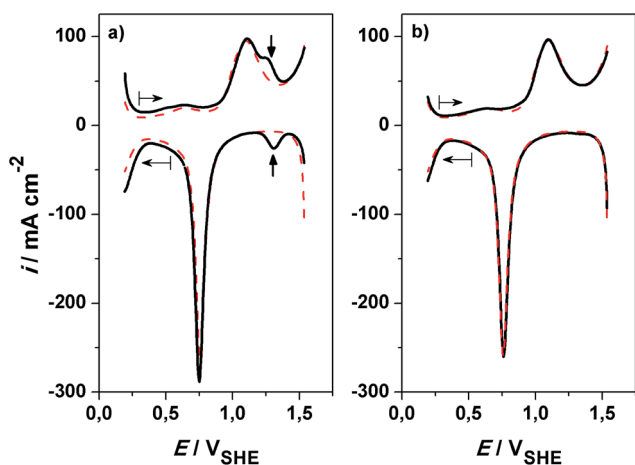


Fig. 1 Differential pulse voltammograms of a bare Au electrode in phosphate buffer with pH 8 solution obtained in the presence of: (a) 0.1 mM  $\text{Ru}(\text{bpy})_3^{2+}$  and (b) 0.1 mM GlyP. In both figures, the red dashed line corresponds to the electrolyte solution blank and the horizontal arrows indicate the potential scan direction.

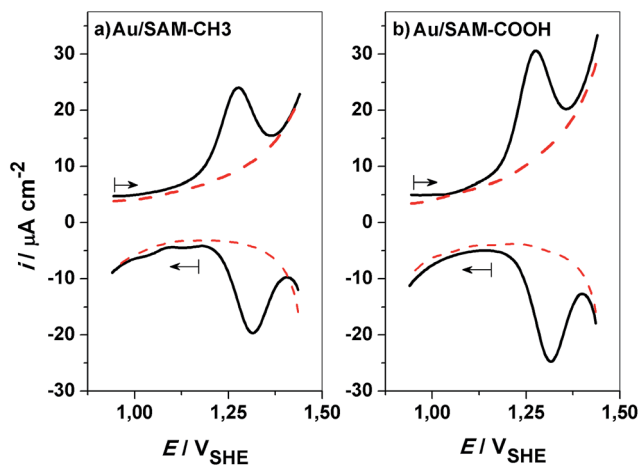


Fig. 2 Differential pulse voltammograms of gold modified electrode. Electrolyte: 0.1 mM  $\text{Ru}(\text{bpy})_3^{2+}$  in pH 8 phosphate buffer (a)  $\text{Au}/\text{SAM}-\text{CH}_3$  (b)  $\text{Au}/\text{SAM}-\text{COOH}$ . In both figures, the red dashed line corresponds to the electrolyte solution blank and the horizontal arrows indicate the potential scan direction.



and the heterogeneous electron transfer rate.<sup>33,34</sup> In addition, an electrostatic attractive interaction between the negatively charged carboxylate terminal groups and the positive  $\text{Ru}(\text{bpy})_3^{2+}$  cation can produce a pre-concentration effect.<sup>35–37</sup> On the other hand, the GlyP oxidation was not detected under the current electrochemical conditions. However, as mentioned above, this was not an essential condition to generate ECL. Then, it was also possible to presuppose that Au/SAM-COOH has the potential to produce an ECL signal in presence of GlyP.

### Electrochemiluminescence characterization

First, the ECL signal was recorded as a function of time for the  $\text{Ru}(\text{bpy})_3^{2+}$ /GlyP system on a bare Au electrode when a potential step between 0.0 and 1.25 V was applied with an amplitude of 0.1 s (Fig. 3a–c). In the absence of GlyP (Fig. 3a), it registered a small ECL background signal, which was associated with the reaction between the electrogenerated  $\text{Ru}(\text{bpy})_3^{2+}$  species and the hydroxyl ion. It is known that this ECL mechanism becomes important in aqueous solutions at pH values above 9.<sup>11,20,29</sup> Moreover, according to the ECL mechanism of the  $\text{Ru}(\text{bpy})_3^{2+}$ /alkylamine system, the deprotonated form of the amine was necessary to be active. Therefore, it was determined that at pH = 8, there is a concentration relationship between  $\text{OH}^-$  and the deprotonated amine that gives the maximum ECL signal.<sup>11,12</sup> Specifically, for the  $\text{Ru}(\text{bpy})_3^{2+}$ /GlyP system at a glassy carbon electrode it was found a similar behaviour with the pH than for  $\text{Ru}(\text{bpy})_3^{2+}$ /alkylamine, which shows also a maximum ECL intensity at pH 8.0.<sup>20</sup>

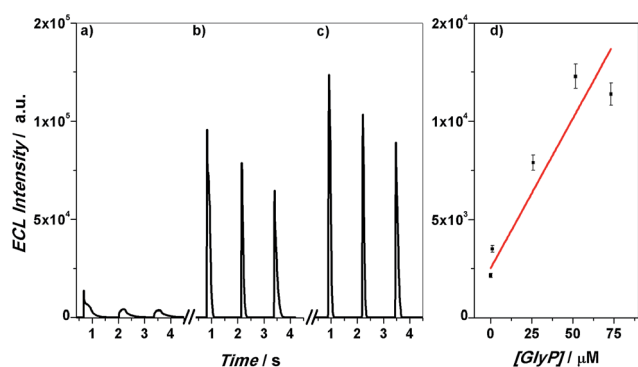


Fig. 3 ECL intensity vs. time for a potential jump between 0 and 1.25 V to a bare Au electrode. Electrolyte: 0.1 mM  $\text{Ru}(\text{bpy})_3^{2+}$  in pH 8 phosphate buffer. (a) Without GlyP. (b) 25  $\mu\text{M}$  GlyP. (c) 100  $\mu\text{M}$  GlyP. (d) Calibration curve for GlyP detection.

On the other hand, when the GlyP was increased systematically from 0 to 100  $\mu\text{M}$  at 0.1 mM of  $\text{Ru}(\text{bpy})_3^{2+}$ , it was observed (see Fig. 3b–d) that the ECL signal was sensitive to the GlyP concentration changes. The fact that the ECL became detectable, when the applied potential was close to the oxidation of  $\text{Ru}(\text{bpy})_3^{2+}$ , implied that the GlyP electrochemical oxidation does not participate in the ECL initiation step. This is in agreement with the mechanism proposed by Jin *et al.* for the same system on glassy carbon (see Scheme 1).<sup>20</sup> However, as shown in Fig. 3d, the ECL signal had a poor linear correlation (see Table 1). This behaviour can be due to gold oxide formation, which is known to affect the generation of ECL.<sup>23,38</sup>

Fig. 4 shows the ECL signal as a function of time obtained on the Au/SAM- $\text{CH}_3$  electrode measured in the same conditions than used for bare Au electrode. The applied potential pulse between 0 and 1.25 V represents a situation of compromise between the stability of the SAM- $\text{CH}_3$  and the electrochemical discharge of  $\text{Ru}(\text{bpy})_3^{2+}$ . Fig. 4a–c shows that the ECL signal was sensitive to the GlyP concentration. Accordingly, it can be concluded that GlyP, as already was observed for the unmodified Au electrodes in Fig. 3, can act as a co-reactant in the presence of the Au/SAM- $\text{CH}_3$ /Ru( $\text{bpy})_3^{2+}$  system.

As can be seen in Fig. 5a–d, the Au/SAM-COOH electrode also shows ECL activity in presence of GlyP/Ru( $\text{bpy})_3^{2+}$ . A simple visual comparison between Fig. 3–5 demonstrates that the ECL signal is affected by the nature of the electrode surface.

The effect of the pH on the calibration curves was examined at pH 6, 8 and 10, and the best analytical performance was observed at pH 8. The results of regression analysis and analytical parameters for GlyP in water at pH 8, obtained with the three electrodes studied, are given in Table 1. The data show that the ECL signal linearly increased with the concentration of GlyP in the range of 1 to 100  $\mu\text{M}$ , demonstrated by a residual plot analysis. A better linear fitting with an  $r^2$  of 0.9996 was observed for the Au/SAM-COOH electrode. The Au/SAM-COOH electrode using the described experimental setup, showed the best analytical performance, reaching a lower limit of detection (LOD) of 0.47 mg GlyP per L (2.78  $\mu\text{M}$ ) and a limit of quantification (LOQ) of 1.08 mg GlyP per L (6.42  $\mu\text{M}$ ). In addition, this modified electrode exhibited good measurement stability and reproducibility with a relative standard deviation (RSD) lower than 2.5% for the data obtained for three tests. The World Health Organization and the Environmental Protection Agency US (EPA) recommends a tolerable limit of 0.7 mg GlyP per L (4.14  $\mu\text{M}$ ) for drinking water.<sup>39</sup> Therefore, the Au/SAM-COOH electrode possesses the adequate analytical parameters for the determination of GlyP in water.

Table 1 Analytical parameters for the ECL determination of GlyP on modified electrodes at pH 8

Electrode	Linear regression equation <sup>a</sup>	$r^2$ <sup>b</sup>	LOD <sup>c</sup>	LOQ <sup>d</sup>
Au	$y = (1.34 \pm 0.28) \times 10^2 x + (3.386 \pm 1.179) \times 10^3$	0.8420	46.48	108.09
Au/SAM- $\text{CH}_3$	$y = (0.52 \pm 0.04) \times 10^2 x + (0.431 \pm 0.199) \times 10^3$	0.9770	20.59	47.88
Au/SAM-COOH	$y = (2.07 \pm 0.02) \times 10^2 x + (7.784 \pm 0.106) \times 10^3$	0.9996	2.78	6.42

<sup>a</sup> Average of three determinations considered.  $y$ : ECL integrated signal.  $x$ : GlyP concentration ( $\mu\text{M}$ ), standard deviation ( $\pm\text{RSD}$ ). <sup>b</sup> Correlation coefficient. <sup>c</sup> LOD ( $\mu\text{M}$ ) calculated using  $3 \times \text{SD}$  of the blank ( $n = 3$ ).<sup>40</sup> <sup>d</sup> LOQ ( $\mu\text{M}$ ) calculated using  $10 \times \text{SD}$  of the blank ( $n = 3$ ).<sup>40</sup>





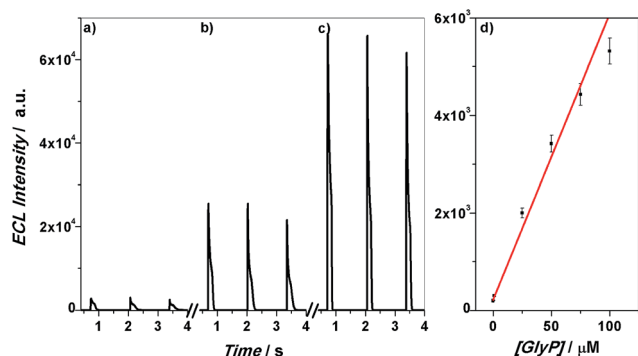


Fig. 4 ECL intensity vs. time for a potential jump between 0 and 1.25 V to an Au/SAM-CH<sub>3</sub> electrode. Electrolyte: 0.1 mM Ru(bpy)<sub>3</sub><sup>2+</sup> in pH 8 phosphate buffer. (a) Without GlyP. (b) 25 μM GlyP. (c) 100 μM GlyP. (d) Calibration curve for GlyP detection.

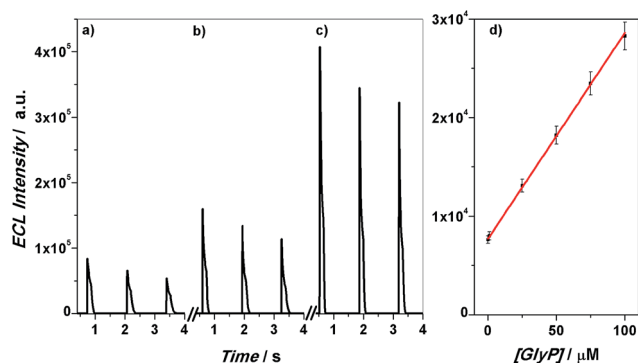
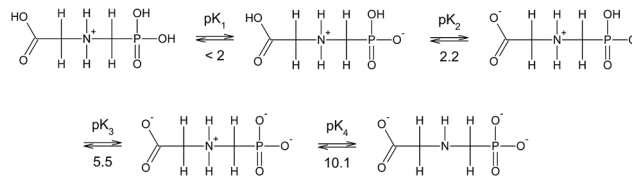


Fig. 5 ECL intensity vs. time for a potential jump between 0 and 1.25 V to an Au/SAM-COOH electrode. Electrolyte: 0.1 mM Ru(bpy)<sub>3</sub><sup>2+</sup> in pH 8 phosphate buffer. (a) Without GlyP. (b) 25 μM GlyP. (c) 100 μM GlyP. (d) Calibration curve for GlyP detection.

It is known that alkyl amine derivatives co-reactants have an oxidation process that is very sensitive to the electrode surface condition. In particular, the oxidation rate of tri-*n*-propylamine (TPrA), which has been widely studied, significantly depends on the nature of the electrode materials.<sup>11,23</sup> Zu *et al.* examined the effect of the electrode's hydrophobic-hydrophilic nature by modifying gold and platinum electrodes with different terminal groups alkylthiol-monolayers on the ECL behavior of the Ru(bpy)<sub>3</sub><sup>2+</sup>/TPrA system.<sup>11,23,41</sup> It was shown that the kinetics of the TPrA anodic oxidation were faster on hydrophobic surfaces, which resulted in a significant increase in the ECL intensity regarding the hydrophilic modified electrode. This behaviour was interpreted through a hydrophobic interaction that allowed the close approach and reorganization of neutral TPrA molecules with the alkanethiol layer on the electrode surface, which facilitated the heterogeneous electron transfer. As it was proposed for TPrA, the GlyP active species in the ECL mechanism had their amine moieties in the deprotonated form (see step 2, Scheme 1). However, while TPrA in its deprotonated form is uncharged, GlyP is negatively charged (see Scheme 2).<sup>12,23,42,43</sup>

As shown in Scheme 1, the heterogeneous electrochemical oxidation of GlyP does not participate in the ECL process.



Scheme 2 GlyP acid-base equilibria.

Therefore, the ECL improvement observed for the Au/SAM-CH<sub>3</sub>/Ru(bpy)<sub>3</sub><sup>2+</sup>/GlyP system regarding unmodified Au/Ru(bpy)<sub>3</sub><sup>2+</sup>/GlyP (see, Table 1) cannot be associated only to the hydrophobic and electrostatic interactions between the SAM and GlyP, as was proposed for TPrA.<sup>12,23,41</sup> Moreover, the enhancement of the ECL signal observed for the Au/SAM-CH<sub>3</sub> electrodes was due to the capabilities of the SAM to avoid the formation of the metal oxide, which affected the interfacial electrochemical electron-transfer kinetics.<sup>23,33-37</sup> This fact was clear when the Ru(bpy)<sub>3</sub><sup>2+</sup> oxidations on the bare and modified electrodes are compared in Fig. 1 and 2. In addition, the presence of SAM on the electrode surface decreased the quenching of the excited state in the proximity of metallic surfaces,<sup>44,45</sup> and also acted as a physical barrier for the adsorption of GlyP oxidation products where both processes positively improved the ECL generation. On the other hand, the Au/SAM-COOH/Ru(bpy)<sub>3</sub><sup>2+</sup>/GlyP system had a better analytical performance than Au/SAM-CH<sub>3</sub>/Ru(bpy)<sub>3</sub><sup>2+</sup>/GlyP. This modified electrode holds a binary SAM, which is composed of an alkylthiol chain that can affect the Ru(bpy)<sub>3</sub><sup>2+</sup>/GlyP in the same way as the Au/SAM-CH<sub>3</sub>; however, it also has a terminal carboxylic acid group that at pH 8 can electrostatically interact with the positive charged Ru(bpy)<sub>3</sub><sup>2+</sup>. As was described in the electrochemical section and shown in Fig. 2, this interaction can produce a pre-concentration effect, which increments the current density with the concomitant enhancement of ECL emission.

A few quantification methods of GlyP using ECL have been reported in the literature, showing detection limits from the nM to μM range.<sup>13-19</sup> The technique established in this study is also in this range. However, the obtained results prove the viability to detect GlyP by ECL using SAM modified electrodes. Moreover, through chemical engineering of the electrode surface, the GlyP analytical signal was improved. In this way, this study opens the possibility to study specific interactions between the SAM and the analyte that can contribute to the improvement of the selectivity and the detection limit.

## Conclusions

The ECL behaviour of the GlyP/Ru(bpy)<sub>3</sub><sup>2+</sup> system on gold electrodes modified with self-assembled monolayers was studied with the aim of applying such findings to the quantification of GlyP without previous chemical derivatization. The ECL response was analysed on three different electrode surfaces, bare gold and alkyl-thiol monolayers with an ionizable (-COOH) and a non-ionizable terminal group. It was found that the modification of the gold electrodes by a SAM-containing



carboxylic end-group enhanced the ECL response for the GlyP/Ru(bpy)<sub>3</sub><sup>2+</sup> system and also exhibited the best analytical performance reaching a limit of quantification (LOQ) for GlyP of 6.42 μM. The use of SAM provides a tool to enhance the sensitivity of ECL sensors, with the potential to be extended to other amine-based herbicides.

## Acknowledgements

The authors gratefully acknowledge the financial support provided by the Consejo Nacional de Investigaciones Científicas y Técnicas (CONICET), Agencia Nacional Científica y Tecnológica (ANPCyT-FONCyT) and Universidad Nacional de Río Cuarto (UNRC). GMM and FF are permanent research fellows of CONICET.

## References

- 1 E. Gregorich, H. H. Janzen, B. Helgason and B. Ellert, *Adv. Agron.*, 2015, **132**, 39–74.
- 2 The Emissions Gap Report 2013, United Nations Environment Programme (UNEP), Nairobi, 2013, accessed February 2017, <http://www.unep.org/emissionsgapreport2013/>.
- 3 *No-Till Farming: Effects on Soil, Pros and Cons and Potential*, ed. E. T. Nardali, Nova Science Publishers, 2010.
- 4 M. Benbrook, *Env. Sci. Eur.*, 2016, **28**(3), 1–15.
- 5 Report National Commission of Inquiry into Agrochemicals, The National Scientific and Technical Research Council, Ministry of Health, Argentina, Buenos Aires, 2009, accessed February 2017, <http://www.msal.gob.ar/agroquimicos/pdf/INFORME-GLIFOSATO-2009-CONICET.pdf>.
- 6 M. Kusters and M. Gerhartz, *J. Sep. Sci.*, 2010, **33**(8), 1139–1146.
- 7 H. S. S. Sharma, E. Carmichael and D. McCall, *Vib. Spectrosc.*, 2016, **83**, 159–169.
- 8 R. Raina-Fulton, *J. AOAC Int.*, 2014, **97**(4), 965–977.
- 9 R. Bataller, I. Campos, N. Laguarda-Miro, M. Alcañiz, J. Soto, R. Martínez-Mañez, L. Gil, E. García-Breijo and J. Ibáñez-Civera, *Sensors*, 2012, **12**(12), 17553–17568.
- 10 J. D. Byer, J. Struger, P. Klawunn, A. Todd and E. Sverko, *Environ. Sci. Technol.*, 2008, **42**(16), 6052–6057.
- 11 W. Miao, *Chem. Rev.*, 2008, **108**(7), 2506–2553.
- 12 *Electrogenerated Chemiluminescence*, ed. A. J. Bard, Marcel Dekker, Inc., New York, 2004.
- 13 J. S. Ridlen, G. J. Klopp and T. A. Niemana, *Anal. Chim. Acta*, 1997, **341**(2–3), 195–204.
- 14 H.-Y. Chuang, T.-P. Hong and C.-W. Whang, *Anal. Methods*, 2013, **5**(21), 6186–6191.
- 15 Q. Cai, X. Chen, B. Qiu and Z. Lin, *Chin. J. Chem.*, 2011, **29**(3), 581–586.
- 16 C.-C. Hsu and C.-W. Whang, *J. Chromatogr. A*, 2009, **1216**(49), 8575–8580.
- 17 H.-Y. Chiu, Z.-Y. Lin, H.-L. Tu and C.-W. Whang, *J. Chromatogr. A*, 2008, **1177**(1), 195–198.
- 18 Q. Zhang, G. Xu, L. Gong, H. Dai, Y. Li and Y. Lin, *Electrochim. Acta*, 2015, **186**, 624–630.
- 19 A. Habekost, *Talanta*, 2017, **162**, 583–588.
- 20 J. Jin, F. Takahashi, T. Kaneko and T. Nakamura, *Electrochim. Acta*, 2010, **55**(20), 5532–5537.
- 21 D. Mandler and S. Kraus-Ophir, *J. Solid State Electrochem.*, 2011, **15**, 1535–1558.
- 22 I. Choi and W.-S. Yeo, *ChemPhysChem*, 2013, **14**(1), 55–69.
- 23 G. Valenti, A. Fiorani, H. Li, N. Sojic and F. Paolucci, *ChemElectroChem*, 2016, **3**(12), 1990–1997.
- 24 A. J. Bard and L. R. Faulkner, *Electrochemical Methods: Fundamentals and Applications*, John Wiley & Sons Inc., New York, 2nd edn, 2000.
- 25 T. Kakiuchi, M. Iida, N. Gon, D. Hobara, S.-I. Imabayashi and K. Niki, *Langmuir*, 2001, **17**(5), 1599–1603.
- 26 Y. F. Xing, S. F. Y. Li, A. K. H. Lau and S. J. O'Shea, *J. Electroanal. Chem.*, 2005, **583**(1), 124–132.
- 27 L. D. Burke, M. M. McCarthy and M. B. C. Roche, *J. Electroanal. Chem.*, 1984, **167**(1–2), 291–297.
- 28 L. D. Burke and P. F. Nugent, *Gold Bull.*, 1997, **30**(2), 43–53.
- 29 P. Pastore, D. Badocco and F. Zanon, *Electrochim. Acta*, 2006, **51**(25), 5394–5401.
- 30 H. Shen, J. E. Mark, C. J. Seliskar, H. B. Mark Jr and W. R. Heineman, *J. Solid State Electrochem.*, 1997, **1**(2), 148–154.
- 31 E. Sabatini and I. Rubinstein, *J. Phys. Chem.*, 1987, **91**(27), 6663–6669.
- 32 C. A. Widrig, C. Chung and M. D. Porter, *J. Electroanal. Chem.*, 1991, **310**(1–2), 335–359.
- 33 P. K. Eggers, D. B. Hibbert, M. N. Paddon-Row and J. J. Gooding, *J. Phys. Chem. C*, 2009, **113**(20), 8964–8971.
- 34 J. M. Campina, A. Martins and F. Silva, *J. Phys. Chem. C*, 2009, **113**(6), 2405–2416.
- 35 J. J. Calvente, G. López-Pérez, P. Ramírez, H. Fernández, M. A. Zón, W. H. Mulder and R. Andreu, *J. Am. Chem. Soc.*, 2005, **127**(17), 6476–6486.
- 36 J. M. Campiña, A. Martins and F. Silva, *J. Phys. Chem. C*, 2007, **111**(14), 5351–5362.
- 37 R. S. Freire and L. T. Kubota, *Electrochim. Acta*, 2004, **49**(22–23), 3795–3800.
- 38 Y. Zu and A. J. Bard, *Anal. Chem.*, 2000, **72**(14), 3223–3232.
- 39 National Primary Drinking Water Regulation, United States Environmental Protection Agency, EPA 816-F09-004, May 2009.
- 40 G. L. Long and J. D. Winefordner, *Anal. Chem.*, 1983, **55**(7), 713A–724A.
- 41 Y. Zu and A. J. Bard, *Anal. Chem.*, 2001, **73**(16), 3960–3964.
- 42 C. N. Albers, G. T. Banta, P. E. Hansen and O. S. Jacobsen, *Environ. Pollut.*, 2009, **157**(10), 2865–2870.
- 43 B. C. Barja and M. Dos Santos Afonso, *Environ. Sci. Technol.*, 1998, **32**(21), 3331–3335.
- 44 S. Zanarini, E. Rampazzo, D. Bich, R. Canteri, L. Della Ciana, M. Marcaccio, E. Marzocchi, M. Montalti, C. Panciatichi, C. Pederzoli, F. Paolucci, L. Prodi and L. Vanzetti, *J. Phys. Chem. C*, 2008, **112**(8), 2949–2957.
- 45 Y. S. Obeng and A. J. Bard, *Langmuir*, 1991, **7**(1), 195–201.

